

Analysis of Long-Term Chlorophyll Trends in Utah Lake using Landsat Data and Lake Regions

Kaylee Brook Tanner
Civil and Construction Engineering,
Brigham Young University
Provo, Utah, USA
ORCID: 0000-0002-4408-8986

Anna Catherine Cardall
Chemical Engineering,
Brigham Young University
Provo, Utah, USA
ORCID: 0000-0001-6962-2142

Gustavious Paul Williams
Civil and Construction Engineering,
Brigham Young University
Provo, Utah, USA
ORCID: 0000-0002-2781-0738

Abstract—Understanding long-term trends in water quality is essential for effective and sustainable management of waterbodies. Using remotely-sensed data, we generated and analyzed a 40-year history of estimated chlorophyll-a (chl-a) concentrations on Utah Lake, which experiences intense algal blooms and is currently the subject of significant controversy over potential remediation strategies. To investigate the potential impacts of shoreline development and WWTP effluent streams on chl-a concentration, which is an indicator of algal biomass, we compared trends and average concentration estimates for different regions of the lake. For the majority of the lake, there is a very small, statistically significant decreasing trend in chl-a concentrations over the last 40 years, and regions receiving WWTP effluent show little difference from regions with undeveloped shoreline. One region (a shallow bay isolated from the rest of the lake) has both higher average concentrations and a significant positive trend over the 40 years, and appears to be influencing the areas of the lake connected to it. These results indicate that other factors besides nutrient inflows are likely driving algal blooms on Utah Lake, and further research is necessary to understand the lake processes and characteristics that influence these blooms.

Keywords— (remote sensing, Landsat, algal blooms, chlorophyll-a, Utah Lake, water quality)

I. UTAH LAKE

Utah Lake is a unique and valuable natural resource in the semi-arid Utah Valley. Shallow, turbid, eutrophic, and slightly saline, the lake degrades and stabilizes pollution well because of its well-oxygenated, high pH waters [1]. It supports and harbors abundant wildlife as part of a productive ecosystem. The lake provides and supports a wide range of beneficial uses, including ecological habitats, water storage, and recreation (e.g., boating, sailing, fishing, and hunting) [2]. The lake is approximately 40 km (24 miles) by 21 km (13 miles) and at maximum fill has a surface area of about 390 km² (96,600 acres), although the average depth of the lake is only about 3 m (9 feet) [3].

Potentially harmful algal blooms (HABs) have closed Utah Lake beaches every summer since 2016 [4] and raised concerns over the health of the lake ecosystem. HABs, which are excessive algal growth that can cause hypoxic and/or toxic water conditions [5], have numerous detrimental effects on lakes and reservoirs in the United States and throughout the world. They are most prevalent during warm periods, and studies indicate that global climate change could be a catalyst for these blooms as lake and reservoir surface temperatures increase [6]. Utah Lake experiences intense blooms with severe consequences for recreational revenue and downstream agriculture.

The region surrounding Utah Lake has undergone extensive population growth, with a population of approximately 220,000 in 1980 increasing to approximately 640,000 in 2020, according to U.S. Census records—an increase of almost 300%.

Accompanying this population growth have been significant land-use changes in the watershed [7].

By analyzing long-term water quality trends on Utah Lake and in different areas of the lake, we can determine whether algal blooms are occurring more frequently or if specific areas of the lake are behaving differently. We use spatial analysis and statistical analysis to determine if the areas that receive waste water treatment plant (WWTP) inflows have identifiable differences, or if these regions behave similarly to other lake regions. These long-term spatial data and accompanying analyses can provide insight into the impacts of WWTP inflows on Utah Lake water quality and inform the debate over the potential effectiveness of limitations on WWTP inflows. The better we understand historical water quality and algal bloom trends, the better we can select and predict the success of potential mitigation measures.

II. METHODS

A. Satellite Data

We chose to use data from the Landsat series of satellites because of the high spatial resolution (approximately 30m per pixel), the high temporal collection rate (every 16 days), large dataset (37 years of data), and the selection of spectral bands designed for vegetation studies [8]. Landsat data has been previously used to evaluate Utah Lake and other lakes in Northern Utah [9, 10]. We used images from the Landsat 5, 7, and 8 missions and the Google Earth Engine (GEE) platform, which simplifies the work required to access and process the images [9, 11], to conduct this analysis.

There are a number of Landsat data products (i.e., processed data) provided by NASA, including surface reflectance data, that have been corrected for sensor calibration and various atmospheric effects to produce images that accurately represent conditions at the earth's surface. These collections eliminate the need for image calibration before processing, and are readily accessible through GEE.

The NASA-processed surface reflectance image collections we used contain a Quality Assessment (QA) band, which flags pixels that are heavily clouded, have cloud shadows, or are otherwise contaminated. We used this band to create pixel quality masks that exclude impaired pixels from the analysis.

B. Chlorophyll Model

For this study we used the Utah Lake-specific chlorophyll-a (chl-a) models developed by Hansen, et al. [12] and Hansen, et al. [13]. We used pixel quality masks based on the QA band, and other models, such water masks, as described by Cardall, et al. [9]. For this study, we used the late season model for Utah Lake shown in Equation 1 [14].

$$\text{chl-a} = e^{(7.33 - 0.004b_1 - 0.05\frac{b_2}{b_7} + 0.01\frac{b_3}{b_5})} \quad (1)$$

This equation computes the estimated concentration of chl-*a* in $\mu\text{g/L}$ for each pixel of water in the image.

C. Trend Analysis Methods

After exporting chl-*a* concentration estimates from GEE, we used the Mann-Kendall (M-K) test to determine the magnitude of any temporal trend in chl-*a* concentrations and whether the trend was statistically significant [15]. The M-K test is a non-parametric statistical test, meaning it is not affected by missing data or the data distribution, so the M-K test does not require any assumptions about data spacing or distributions. The M-K test is recommended by the US EPA National Nonpoint Source Monitoring Program for trend analysis [16]. To perform the M-K test, we used the `pymannkendall` package (ver 1.4.2), from `conda-forge` [17].

The M-K test null hypothesis, H_0 , is that the data come from a population with independent realizations and are identically distributed. The alternative hypothesis, H_A , is that the data follow a monotonic trend. The Mann-Kendall test statistic is calculated according to:

$$S = \sum_{k=1}^{n-1} \sum_{j=k+1}^n \text{sgn}(X_j - X_k) \quad (2)$$

With:

$$\text{sgn}(X_j - X_k) = \begin{cases} 1 & \text{if } (X_j - X_k) > 0 \\ 0 & \text{if } (X_j - X_k) = 0 \\ -1 & \text{if } (X_j - X_k) < 0 \end{cases} \quad (3)$$

Where S is the M-K statistic, n is the number of samples, and X_i is the i^{th} sample. The M-K test evaluates every potential pair of measurements and sums the sign of the difference. A positive S value indicates that measured values later in the series tend to be larger than measured values earlier in the series, indicating an upward trend. A negative S value indicates that later values tend to be smaller than earlier values, indicating a downward trend. A small absolute value of S indicates no trend. There are several test statistics which can be computed for the M-K test; we chose to compare the p value to a significance level of 0.05 to determine if the trend was significant. We estimated the rate-of-change or slope using both the Sen slope estimator [18] and a fitted linear regression line in units of $\mu\text{g/L/year}$.

III. UTAH LAKE REGIONS AND ANALYSIS

To attempt to separate the impacts of WWTPs, river inflows, and other spatially heterogeneous influences on Utah Lake, we divided the lake into several different regions for statistical analysis (Table 1 and Figure 3). We selected these regions to isolate various inflows, outflows, and shoreline land uses. In addition to these regions, we computed the statistics for the entire lake.

When computing chl-*a* concentrations for any image, only the pixels that were not masked were used. We used two masks. The first was a water mask to only select pixels that contained water as the shoreline changes with lake level. The next mask was based on the pixel quality band provided with the image (this band identifies pixels that are contaminated with clouds, cloud shadows, or have sensor errors). This means that the size of the regions that contain shoreline, as well as the entire lake, changed with time as the lake level

changed, resulting in a different number of pixels in each image in the time series. When computing statistics for a region, only the pixels within the region that were not masked were used.

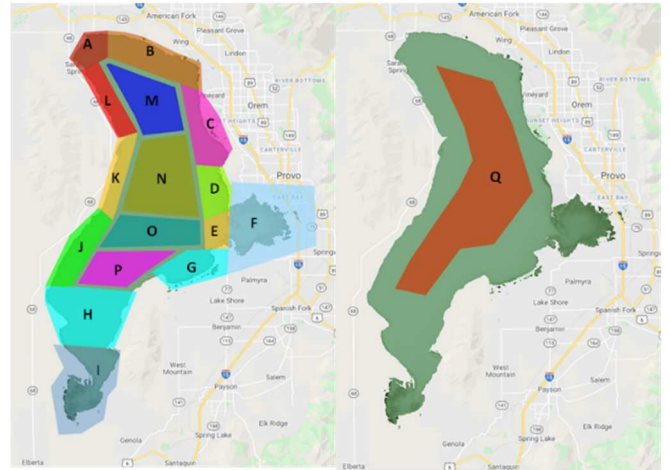


Fig. 1. Utah Lake regions for statistical analysis. These include the smaller regions in the left panel (regions A through P) and a lake center region shown in the right panel (region Q). In addition, we computed statistics for the entire lake.

Region A contains the Jordan River outlet. This is the only outlet for Utah Lake. Most of the north and east shoreline areas (regions B and C) are pasture or swamp lands and contained the Geneva Steel plant, which is being decommissioned. Region B contains both the American Fork and Lindon Marinas, and the shoreline there is relatively undeveloped. Housing development in Region C started 5 – 10 years ago; prior to that the area was agricultural and pastureland. Region D contains Provo Harbor, the most active marina on the lake, and the discharge point for the Provo River, which is the main tributary to the lake. About 2 years ago, restoration construction on the Provo River outlet commenced, and it is almost complete. The shoreline in this region includes a state park and some developed land. Provo Bay (Region F) exhibits different characteristics from the rest of the lake, it is less turbid and surrounded by wetlands, and becomes extremely shallow during drought years. It receives inflow from Hobbles Creek and several other small streams. The Provo and Springville WWTPs discharge into Provo Bay. About 10 years ago, the Hobbles Creek restoration altered the flow patterns, allowing Hobbles Creek to discharge directly into the bay without flowing through wetland vegetation. Region E, at the mouth of Provo Bay, also exhibits slightly different characteristics from the lake, with less turbid water as the discharge from Provo Bay enters the lake. Region G is pastureland on the shore with little development. It receives discharge from the Spanish Fork WWTP. Region H is the southern portion of the lake. The shore in this area contains some pastureland on the east, with the central portion containing orchards. The western shore is a dry desert landscape. This region contains numerous seeps and springs. One large spring creates Bird Island, a carbonate deposit actively maintained, about 1 mile offshore. The lakebed between the shore and Bird Island is a hard carbonate substrate with shallow water (<1m) in many areas. The region J shoreline is a desert landscape with little to no development and no streams or seeps, though there might be seeps in the lake. Region K is a desert landscape, like region J, but in the last 10 – 15 years housing development has occurred with

housing very near the shore. Region L has some seeps springs, but no streams or creeks. The small town of Saratoga Springs is in this region. Recently, in the last 15-20 years, this area has been significantly developed with housing close to the shore. Regions M, N, O, and P represent center sections of the lake away from shoreline influences. Region Q represents the entire center of the lake.

TABLE I. UTAH LAKE ANALYSIS REGIONS

Name	Letter	Major inflows, outflows, and notes
Jordan River	A	Jordan River outlet.
North Shore	B	TSSD WWTP outfall. Historic Geneve Steel Outfall; American Fork and Lindon Marinas.
NE Shore	C	Orem WWTP outfall.
E Central Shore	D	Provo River inlet Provo Harbor
Provo Bay Mouth	E	Provo Bay inflow
Provo Bay	F	Hobble Creek inflow
SE Shore	G	Provo and Springville WWTPs outfall Several seeps, springs, and small creeks. Spanish Fork WWTP outfall.
Southern Lake	H	Several seeps and groundwater discharge points. Warm springs in the lake.
Goshen Bay	I	Very shallow bay.
SW Shore	J	No continuous discharges
W Central Shore	K	No continuous discharges. May be seeps
NW Shore	L	Seeps and springs
N Central Lake	M	Northern center lake portion
Mid-N Central	N	Mid-northern lake portion
Mid-Central	O	Mid-center lake portion
S Central Lake	P	South-center lake portion Numerous warm springs in lake
Central Lake	Q	Center lake portion.

IV. RESULTS

A. Trend Analysis

TABLE II. TREND ANALYSIS RESULTS FOR DATA FROM MARCH THROUGH NOVEMBER.

Area	Trend	Sig.	Sen's Slope	Regression Slope	Avg	N
Lake	decreasing	TRUE	-0.03	-0.09	5.09	801
A	decreasing	TRUE	-0.07	-0.18	6.97	735
B	decreasing	TRUE	-0.05	-0.18	7.70	762
C	decreasing	TRUE	-0.10	-0.27	11.19	760
D	decreasing	TRUE	-0.06	-0.00	11.40	759
E	no trend	FALSE	-0.00	0.27	14.25	731
F	increasing	TRUE	0.73	0.94	80.55	764
G	decreasing	TRUE	-0.06	-0.01	12.80	747
H	decreasing	TRUE	-0.05	-0.15	6.86	765
I	decreasing	TRUE	-0.27	-0.32	18.36	767
J	decreasing	TRUE	-0.04	-0.19	6.19	758
K	decreasing	TRUE	-0.03	-0.05	4.64	755
L	decreasing	TRUE	-0.03	-0.02	4.80	746
M	decreasing	TRUE	-0.03	-0.04	4.82	765
N	decreasing	TRUE	-0.03	-0.02	4.70	771
O	decreasing	TRUE	-0.03	-0.06	4.89	764
P	decreasing	TRUE	-0.03	-0.09	4.97	765

Q decreasing TRUE -0.03 -0.07 4.02 791

Table II presents the results of the Mann-Kendall test applied to chl-a estimates from March through November for each analysis region. Except for Provo Bay (F) and the mouth of Provo Bay (E), all regions have very small decreasing trends, with Sen's slope values of less than 0.1 $\mu\text{g/L/year}$, showing only minimal changes over the 40-year period. Provo Bay (F) has an increasing trend, and the slope of 0.730 $\mu\text{g/L/year}$ is much larger than any of the other computed slopes. The region at the mouth of Provo Bay (E) shows no trend, with a Sen's slope value of negative 0.001 (decreasing) and a linear regression slope value of positive 0.27 (increasing).

The trends in all regions except the mouth of Provo Bay (E) are statistically significant based on a p value of 0.95; however, all the regions have over 700 data points (i.e., images with pixels in the region) over the nearly 40-year time period, allowing most statistical tests to be significant, even though the very low Sen's slope (and linear regression slope) values indicate there is essentially no trend for all regions except Provo Bay.

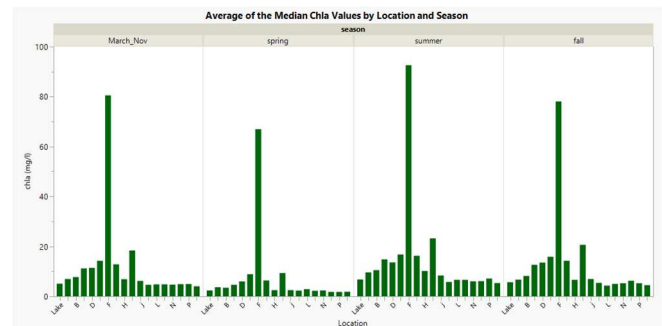


Fig. 2. Seasonal and locational averages of the median chl-a values.

Although the magnitudes of the trends in all regions except Provo Bay are very small, there is noticeable variation in the average chl-a concentrations in different regions. A Kruskal-Wallis multiple comparison of means test on the data from each region gives a p -value of $2.2e-16$, indicating that at least some of the differences in average chl-a concentrations between regions are statistically significant. Figure 2 illustrates the average chl-a values for each region by season, with the first panel representing the entire growing season (March through November), the next panel the spring months (March through May), the next panel the summer months (June through August), and the last panel the fall months (September through November). In each panel, each region is represented by a bar, with the height corresponding to the average chl-a value over that period. The bars are in order, with the entire lake being first, then the shoreline starting at the Jordan River Outlet (A) and continuing clockwise through the NW Shore area (L); next are the areas in the center of the lake starting with the northernmost region (M) and continuing south through area P, with Area Q, the entire central lake, last.

Figure 2 shows that regions F (Provo Bay) and I (Goshen Bay) have the highest average chl-a concentrations. Areas E (Provo Bay Mouth) and G (Southeast Shore) are the next highest and are both near Provo Bay. Areas C (Northeast Shore) and D (East Central Shore) have slightly higher levels and are just north of the Provo Bay entrance in the direction of water flow and prevailing wind.

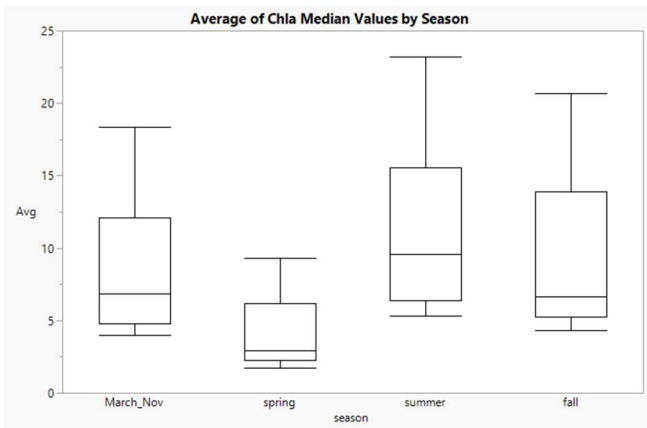


Fig. 3. Box-and-whisker plots showing the seasonal distribution of the average chl-a values for the lake.

Figure 3 shows that the distribution of the average of the median chl-a concentration for the regions changes with season, starting with low values in the spring, increasing in the summer, and decreasing in the fall, but not as low as the initial spring values. The distribution of values for the entire growing season (the March through November time period) is about the same as the fall distribution, though slightly lower.

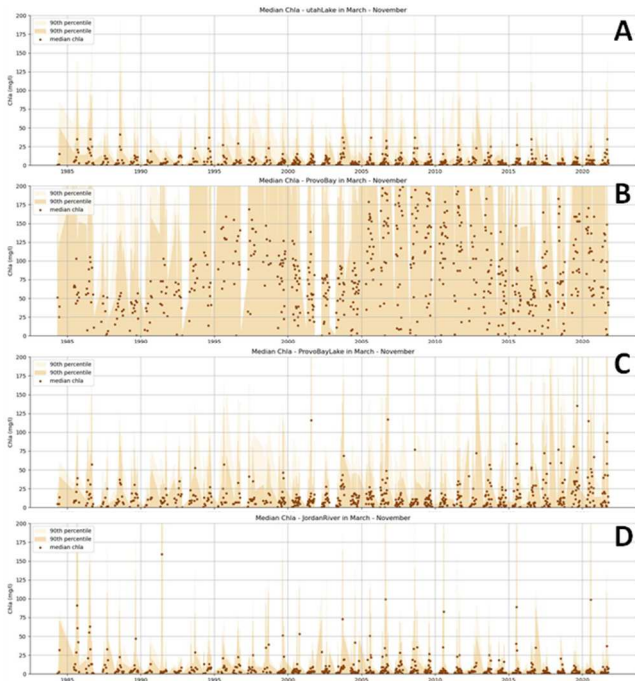


Fig. 4. Median chl-a values from March through November for selected analysis regions: the entire lake (A), Provo Bay (B), Mouth of Provo Bay (C), and the Jordan River Outfall (D).

Figure 4 shows example plots of chl-a concentrations (March through November). We did not include data from the winter months because the chl-a model does not handle pixels with ice and snow well. The plots include the measured values, shown as points, plus the 75th and 90th percentiles shown as a filled backgrounds, to highlight the spread of the data.

V. DISCUSSION

Since the lake is extremely shallow for its size with about 50% of its inflow lost to evaporation [19], spatial mixing within the lake is fairly limited. Because of this, we expected lake regions that received significant amounts of effluent from

WWTPs and regions with significant shoreline development over the last 40 years to show an increasing trend in chl-a concentrations, as population has grown significantly over the study period. These changes are not evident in the data. While there are differences in the average chl-a values for each region, the regions with higher values are all associated with Provo Bay.

Provo Bay does receive the outfalls from the Provo and Springville WWTPs, but these plants combined do not have as much effluent as TSSD, which discharges into Region B (North Shore) and is similar in size to the Orem WWTP which discharges into Region C (NE Shore). The data show that chl-a concentrations in regions of the lake that have experienced development of the shoreline are not significantly different from those that have not. The center of the lake is also similar to the shoreline areas, with the exception of Provo Bay and the regions around Provo Bay.

One potential issue for additional study involves establishing what limits phytoplankton growth in Utah Lake. There is ongoing debate over whether growth is light- or nutrient-limited. Researchers hypothesize that phytoplankton growth is light limited in Utah Lake's extremely turbid water, which has secchi depths on the order of 10 cm (personal data). Some studies indicate that algal growth is light-limited at these turbidity levels [20], and our data support this hypothesis by showing that nutrient inflows do not appear to significantly affect chl-a concentrations. Based on visual analysis of satellite images, Provo Bay has less turbid water. This lack of turbidity may allow more phytoplankton growth in the bay. Water flows from Provo Bay into the lake, which could explain the higher concentrations we found in the regions surrounding the mouth of Provo Bay. The Hobble Creek inflow area to Utah Lake underwent significant restoration in the late 2000s, which decreased the amount of sediment in the Bay and could have impacted turbidity and the effects of light limitation on algal growth.

VI. CONCLUSIONS

We used nearly 40 years of Landsat data to evaluate trends in chl-a concentrations in Utah Lake. We analyzed data from March through November, as ice and snow on the lake impair the accuracy of satellite measurements of chl-a. We separated the lake into 12 different regions, each associated with different inflows, shoreline development conditions, and other differences. We found that chl-a concentrations, with the exception of Provo Bay and the mouth of Provo Bay, show a statistically significant decreasing trend over this period, though the trends are essentially flat: 0.1 $\mu\text{g/L}/\text{year}$ or less. Provo Bay shows a statistically significant increasing trend of 0.73 $\mu\text{g/L}/\text{year}$, while the mouth of Provo Bay does not have a statistically significant trend.

This study supports the theory that inflows and shoreline activities likely have not affected chl-a concentrations in Utah Lake over the last 40 years, a period of significant population growth around the lake. The results suggest further studies to determine if light limitation and turbidity in Provo Bay cause the higher concentrations and increasing trend shown in that region.

Long-term satellite data are a unique resource for investigating the health, history, and processes of fresh water lakes and reservoirs. This study provides water quality managers with information they can use in studying and managing Utah Lake.

REFERENCES

- [1] G. P. Williams, "Great Salt Lake and Utah Lake Statistical Analysis: Vol II: Utah Lake," 2020, vol. 2.
- [2] L. B. Merritt and A. W. Miller, "Interim Report on Nutrient Loadings to Utah Lake: 2016," Jordan River, Farmington Bay & Utah Lake Water Quality Council, Provo, Ut, October, 2016 2016.
- [3] (August, 2007). *Utah Lake TMDL: Pollutant Loading Assessment & Designated Beneficial Use Impairment Assessment - FINAL DRAFT*.
- [4] U. DEQ, "Harmful Algal Blooms Home - Utah Department of Environmental Quality," ed, 2021.
- [5] K. G. Sellner, G. J. Doucette, and G. J. Kirkpatrick, "Harmful algal blooms: causes, impacts and detection," *Journal of Industrial Microbiology and Biotechnology*, vol. 30, no. 7, pp. 383-406, 2003-07-01 2003, doi: 10.1007/s10295-003-0074-9.
- [6] H. W. Paerl and J. Huisman, "Climate change: a catalyst for global expansion of harmful cyanobacterial blooms," *Environmental Microbiology Reports*, vol. 1, no. 1, pp. 27-37, 2009-02-01 2009, doi: 10.1111/j.1758-2229.2008.00004.x.
- [7] E. Call, "Calculating the Impact of ~ 65 years of Anthropogenic Activity on the Utah Lake Watershed Using Remote Sensing and Spatial Modeling," 2019.
- [8] "Landsat—Earth observation satellites," in "Fact Sheet," Reston, VA, Report 2015-3081, 2016. [Online].
- [9] A. Cardall, K. B. Tanner, and G. P. Williams, "Google Earth Engine Tools for Long-Term Spatiotemporal Monitoring of Chlorophyll-a Concentrations," *Open Water Journal*, vol. 7, no. 1, p. 4, 2021.
- [10] C. H. Hansen, "Google Earth Engine as a Platform for Making Remote Sensing of Water Resources a Reality for Monitoring Inland Waters," presented at the World Environmental and Water Resources, Austin, TX, May 17-25, 2015.
- [11] C. Hansen, *Google Earth Engine as a Platform for Making Remote Sensing of Water Resources a Reality for Monitoring Inland Waters*. 2015.
- [12] C. H. Hansen, S. J. Burian, P. E. Dennison, and G. P. Williams, "Evaluating historical trends and influences of meteorological and seasonal climate conditions on lake chlorophyll a using remote sensing," *Lake and Reservoir Management*, vol. 36, no. 1, pp. 45-63, 2020-01-02 2019, doi: 10.1080/10402381.2019.1632397.
- [13] C. H. Hansen, S. J. Burian, P. E. Dennison, and G. P. Williams, "Evaluating historical trends and influences of meteorological and seasonal climate conditions on lake chlorophyll a using remote sensing," *Lake and Reservoir Management*, vol. 36, no. 1, pp. 45-63, 2020.
- [14] C. H. Hansen and G. P. Williams, "Evaluating Remote Sensing Model Specification Methods for Estimating Water Quality in Optically Diverse Lakes throughout the Growing Season," *Hydrology*, vol. 5, no. 4, 2018, doi: 10.3390/hydrology5040062.
- [15] H. B. Mann, "Nonparametric Tests Against Trend," *Econometrica*, vol. 13, no. 3, p. 245, 1945-07-01 1945, doi: 10.2307/1907187.
- [16] D. W. Meals, J. Spooner, S. A. Dressing, and J. B. Harcum, "Statistical Analysis for Monotonic Trends," *US EPA: National Nonpoint Source Monitoring Program: Tech Notes*, vol. 6, 2011.
- [17] Anaconda.org. "conda-forge / packages / pymannkendall 1.4.2." Anaconda.org.
- [18] D. R. Helsel and R. M. Hirsch, *Statistical methods in water resources*. Elsevier, 1992.
- [19] D. K. Fuhriman, L. B. Merritt, A. W. Miller, and H. S. Stock, "HYDROLOGY AND WATER QUALITY OF UTAH LAKE," *Great Basin Naturalist Memoirs*, no. 5, pp. 43-67, 1981. [Online].
- [20] J. Jones, "Experimental evidence of light and nutrient limitation of algal growth in a turbid midwest reservoir," *Archiv fur Hydrobiologie*, vol. 135, pp. 321-335, 01/01 1996.